Thin film composite optical waveguides for sensor applications: a review

Abliz Yimit[a,b], Axel G. Rossberg[a], Takashi Amemiya[a], Kiminori Itoh[a,*]

[a] *Graduate School of Environment and Information Sciences, Yokohama National University, Tokiwadai, Hodogaya-ku, Yokohama 240-8501, Japan*
[b] *College of Chemistry and Chemical Engineering, Xinjiang University, Xinjiang Urumqi 830046, PR China*

Abstract

We review the design and fabrication of thin-film composite optical waveguides (OWG) with high refractive index for sensor applications. A highly sensitive optical sensor device has been developed on the basis of thin-film, composite OWG. The thin-film OWG was deposited onto the surface of a potassium-ion-exchanged (K^+) glass OWG by sputtering or spin coating (5–9 mm wide, and with tapers at both ends). By allowing an adiabatic transition of the guided light from the secondary OWG to the thin-film OWG, the electric field of the evanescent wave at the thin film was enhanced. The attenuation of the guided light in the thin film layer was small, and the guided light intensity changed sensitively with the refractive index of the cladding layer. Our experimental results demonstrate that thin-film, composite OWG gas sensors or immunosensors are much more sensitive than sensors based on other technologies.
© 2004 Elsevier B.V. All rights reserved.

Keywords: Composite optical waveguide; Thin film; Biochemical sensors; Refractive index sensor

1. Introduction

A typical planar optical waveguide (OWG) consists of a substrate and a thin top layer (waveguide layer) with refractive index larger than that of the substrate; the covering material (clad) is usually air. An interesting feature of such waveguides is that the electric field associated with a light-wave propagating in the waveguide layer is very strong at the surface of the OWG; hence, highly sensitive optical monitoring can be performed for chemical species located at the OWG surface on the basis of absorption and scattering of the guided light. For instance, laser flash photolysis [1], and spectroelectrochemistry [2] have been applied to surface species using OWGs. The first OWG sensor has been described in 1980s [3,4]. A highly sensitive OWG biochemical sensor was constructed using grating couplers [5].

Methods for fabricating OWGs are solution-phase, deposition, and ion exchange process. For solution phase fabrication, doctor blading, spin coating, dip coating, and horizontal-flow coating are used. In all of these methods, a solid-phase organic (or inorganic) material is dissolved in an appropriate solvent and then deposited on an optical quality substrate. Methods for deposit fabrication are sputtering and vapor deposition. The sputter process uses an rf-heated target as the source of thin-film atoms, which diffuse to the substrate. The thickness of the thin film grown onto the substrate is controlled largely by the duration of the process; however, other factors that affect deposition include ambient pressure and temperature. The solution and deposition processes described above produce step-index guiding films where the substrate and waveguide boundary have an abrupt change in refractive index. Conversely, ion-exchange methods produce a graded-index waveguide that has a gradual transition from the substrate to the waveguide refractive index. This is accomplished by exchanging mobile or

weakly bound ions in a solid with other ions from an external source, such as exchanging Na^+ in soda lime glass with K^+ by immersing the substrate in molten KNO_3 at 365 °C. The net index variation depends on the ionic polarizability, molar volume, and the stress state created by the substitution. In the case of K^+–Na^+ exchange, as the polarizability of K^+ ions is much lager than that of Na^+ ion in the glass, the surface refractive index change is at least $\Delta n \geq 0.01$ [6].

Recently, thin-film OWG sensors for gaseous analytes based on porous glass materials, prepared by the sol–gel process, have been described [7–9]. Ion-sensitive and selective thin-film (polymer) waveguide sensors have been reported [10,11]; and a polymer waveguide sensor with symmetric multilayer configuration was fabricated and its application in sensing low humidity concentration has been demonstrated [12]. However, this kind of thin-film OWG sensor has a relatively low sensitivity, probably due to an increased scattering loss arising from a nonuniform distribution of the thin film in the guiding layer. It is well known that a large scattering loss often makes OWG chemical sensors incapable of working effectively.

Compared to other OWGs, ion-exchanged glass OWGs are easily prepared and their good optical and mechanical qualities at low cost are attractive. In particular, they are known to show a low loss (>0.1 dB cm^{-1}). However, for the use as chemical sensors, their sensitivity is relatively low [13,14].

In our laboratory, the use of the slide glass OWG for (bio-) chemical sensing began in 1988 [1,2]. However, the weak evanescent field turned out to be a big drawback of the slide glass OWGs for (bio-) chemical sensing applications. It was found to be a direct result of the graded-index waveguiding layer, and implies a low sensitivity for most of the sensing applications.

For improving the sensitivity of glass OWG-based (bio-) chemical sensor, we proposed a method to enhancing the evanescent field in 1991 [14,15]. A composite OWG is composed of a tapered thin film of high refractive index locally coated on a K^+-ion-exchanged glass planar waveguide. The use of composite OWG for (bio-) chemical sensing applications was new at that time. Later, we fabricated the Ag^+/K^+-ion-exchanged glass composite OWG [16,17], TiO_2 film/K^+ [18] and polytungstic acid (PTA) thin-film/K^+-ion-exchanged glass composite OWG [19], that clearly demonstrated the advantages of the composite thin-film structure. In an application to ammonia gas sensors [20–23], ammonia at concentrations of one part per trillion (ppt) were easily detected. As a biochemical application the detection of immonuglobulin G at concentrations of 70 pg/cm^3 was demonstrated [24].

In this paper, we give an overview over the new thin-film composite OWG system made from thin films and ion-exchanged OWGs, and show that they have extremely high sensitivity at reasonably low loss.
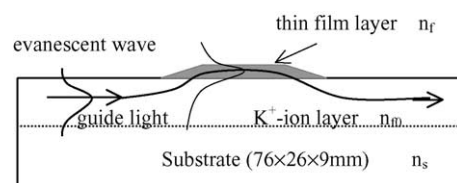

Fig. 1. Structure of the composite OWG and the principle of operation. n_s, n_{f0}, and n_f are respectively, refractive index of the substrate (1.515), the K^+-ion-exchanged layer (1.5195), and of the thin film.

2. The composite optical waveguide

2.1. Structure of the composite OWG and tapered velocity couplers

We had shown in previous work that high sensitivity can be obtained with thin-film OWGs made of materials having high refractive index [1,17]. But the propagation loss of these OWGs was too large to use them in sensor fabrication [15]. An effective composite structure was therefore designed to solve this problem. The structure of the composite OWG is shown in Fig. 1. It is usually composed of single-mode K^+-ion-exchanged glass OWG overlaid locally with a high-index thin film that has two slopes (tapered ends). First, the laser beam is injected into the K^+-ion-exchanged glass OWG using some optical coupler (e.g. a prism). The guided light propagates along the glass OWG almost without attenuation. The slopes at the ends of the thin-film OWG serve as tapered velocity couplers, and the guided light will transfer to the thin film and back to the K^+-ion-exchanged glass when an adiabatic condition [25] is fulfilled (Fig. 1). In this composite OWG system, coupling of the laser beam is accomplished at the part of the glass OWG, so that the guided light does not suffer from excess attenuation before reaching the thin-film or the out-coupling coupler. Experimentally it was found that a 90% adiabatic condition is realized at the slope length of 0.5 mm for the 0th mode, and 1 mm for the 1st mode, which is in accord with theoretical estimates [14,15].

2.2. Fabrication of the composite OWG

2.2.1. Composite ion-exchanged OWG

A major limitation for the sensitivity of conventional Ag^+-ion-exchanged OWGs is the large attenuation of propagating light (5–15 dB cm^{-1}), mainly due to the roughness of the OWG surface [17].

Composite glass ion-exchanged OWG overcome this problem by combining a low-loss K^+-ion-exchanged OWG with a highly sensitive Ag^+-ion-exchanged OWG on a glass substrate using a tapered velocity coupler as shown in Fig. 2. Attenuation losses due to surface scattering are here restricted to the comparatively small high-sensitivity region of the surface.

To obtain this structure, a preheated glass substrate (microscope glass slide, size 76 mm × 26 mm × 1 mm) was first
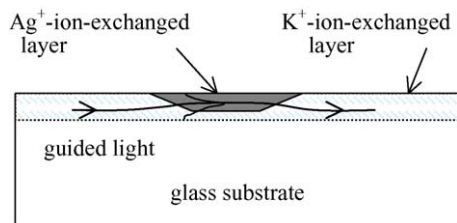
Fig. 2. Structure of the ion-exchanged composite OWG. The arrow shows how the guided light is transferred from one part of the OWG to another part via adiabatic transition [16,17].

dipped into molten KNO_3 at 400 °C for 30 min. Then, a piece of frosted glass (10 mm × 26 mm) covered with a thin layer of $AgNO_3$ mixed with KNO_3 and $NaNO_3$ was fixed onto the K^+-ion-exchanged glass OWG with a clamp, and the whole sample was kept at 300 °C in an electric furnace for 5–90 min. The Ag^+-ion-exchange takes place at the surface of the K^+-ion-exchanged glass OWG, but there is no further diffusion of K^+ ions at this temperature.

2.2.2. Thin-film composite OWG

The conventional fabrication of composite OWGs consists of two steps. First, a single-mode K^+-ion-exchanged glass OWG is prepared (see above). Then, a dielectric thin film with high refractive index is deposited onto the K^+-ion-exchanged glass OWG by radio-frequency (rf) sputtering or solution-phase techniques.

For the preparation of metal oxide thin films, we used the rf sputtering method. To taper the ends (slopes) of the thin films, a mask with a rectangular window was mounted at a distance of several mm from the substrate during sputtering. Fig. 4 shows the setup inside the vacuum chamber of the rf sputtering system. The mask can be made of a metal plate, an alumina ceramic plate, or slide glass. Dielectric materials for the thin film include TiO_2, ZnO, WO_3, and Al_2O_3. For its high refractive index and its strong resistance to acid and alkali, TiO_2, in particular, is an ideal candidate for use in composite OWGs.

The sputtering was carried out in an Ar/O_2 gas mixture (1:1). The incidence rf power used was 250–300 W, and the operation vacuum was about 5×10^{-3} Pa. The temperature of the substrate was kept below 100 °C during the sputtering [18]. For a typical experimental geometry, see Fig. 3a and b. The thickness and refractive index were measured with an ellipsometer after sputtering.

Instead of rf sputtering, spin coating has also been used to obtain the upper thin film. This technique, using amorphous, inorganic compounds, is often employed for applications such as antireflection coatings and also thin-film optical waveguides. For example, peroxopolytungstic acid (PTA), a strong solid acid, is an interesting material not only because of its unique structure [26] but also for is exceptional functional properties: It is a spin-coatable inorganic deep UV resist; and the films have the highest refractive index among spin-coatable amorphous films reported so far (from 1.7 up
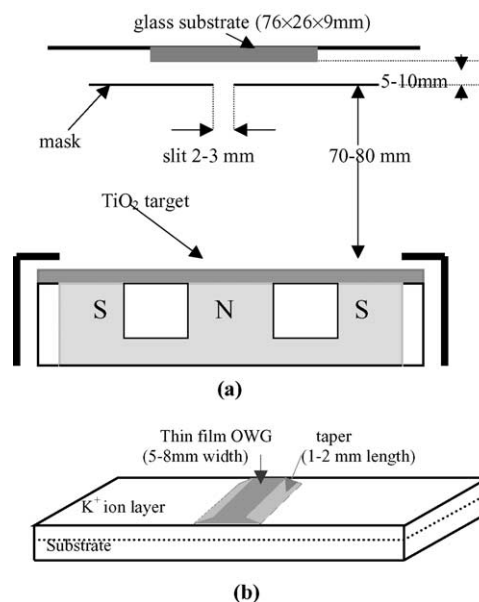

Fig. 3. (a) A mask with a narrow slit of 2–3 mm width was used to form the slops during the sputtering. (b) The thin film sputtered onto the surface of the K^+-ion-exchanged glass optical waveguide [18].

to >2.0 for films dried at 100 °C [27]). PTA, prepared by mixing 3 g tungsten powder into 15 ml of 30% H_2O_2 solution, was dissolved into ethanol (or water), and the solution was deposited onto the substrate, i.e. the K^+-ion-exchanged glass OWG, by spin coating followed by drying at 120 °C [27]. In order to obtain the tapered velocity couplers (slopes), the PTA films were etched with water (pH = 8–8.5). The length of the slope was controlled by changing the speed of immersing the sample into the etchant, and the length of the slope was measured with an optical microscope [19].

2.3. Surface sensitivity of the OWG

To discuss the surface sensitivity of the OWGs, we introduced the relative sensitivity S_{rel} as a measure which represents in how far the OWGs are sensitive compared to conventional optical measurements with normal incidence of the monitoring light beams (see Fig. 4). The value of S_{rel} is defined by the following procedure. First, methylene blue (MB) dye molecules were adsorbed onto the OWG surface
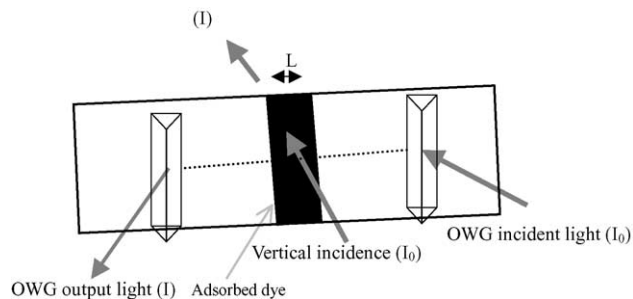

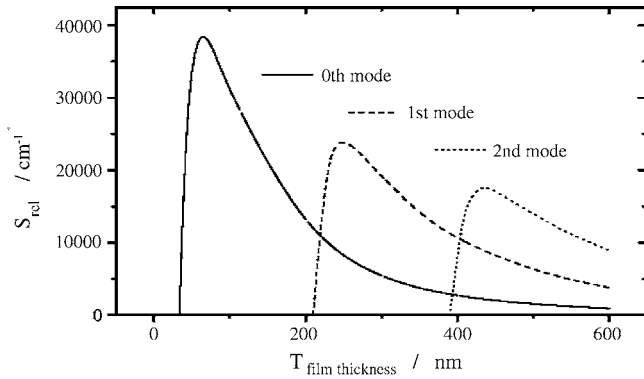Fig. 4. Measurement method for the relative sensitivity of the OWG.

Fig. 5. A typical theoretical the relation between relative sensitivity and the thickness of the waveguide layer (TiO$_2$ thin film). The parameters used in this calculation were $n_f = 2.3$ (TiO$_2$ film), $n_s = 1.515$ (glass), $n_c = 1.0$ (air), and $\lambda = 632.8$ nm.

from an aqueous solution, and optical density of the adsorbed dye (OD$_{ad}$) at 632.8 nm was measured in air using UV–vis spectrophotometer.

Second, OD values were obtained for guided TE (transverse electric) modes from attenuation of the guided light (OD$_{OWG}$). Finally, the relative sensitivity is calculated as $S_{rel} = (OD_{OWG}/OD_{ad})/L$, where L is the path length of the OWG covered with the adsorbed dye molecules. It should be noted that we used TE modes here because relative sensitivity was estimated on the basis of measurements with normal incidence of the monitoring light; that is the electric field of the monitoring light is oscillating parallel to the OWG surface in these two cases [28].

The relative sensitivity (S_{rel}) values obtained above were compared to theoretical (S_{OWG}) ones based on electric field distribution calculated by solving the wave equations [6] numerically with the Runge–Kutta method. In this calculation, n_{sur} was the average surface refractive index defined by $(n_f^2 + n_c^2)^{1/2}$ and N_{eff} was the effective refractive index of the waveguide. By using these parameters, S_{OWG} is expressed as follows [14]:

$$S_{OWG} = (n_{sur}^2/2 \times N_{eff})E_y(0)^2 / \int_{-}^{+} E_y(x)^2 dx \qquad (1)$$

The refractive index of thin-film OWG is given as n_f; that of the cladding layer (usually air, 1.0) n_c. $E_y(x)$ refers to the electric field distribution of the guided light, and $E_y(0)$ in the intensity of the electric field on the surface of OWGs.

Fig. 5 shows an example of calculated relative sensitivity S_{OWG} values for thin-film composite OWGs. The calculation is based on a step structure, that is, a uniform film having a refractive index n_f is coated on a substrate with refractive index n_s; and a uniform cladding layer with refractive index n_c. One can see that S_{OWG} is approximately inversely proportional to the thickness of the film, $S_{OWG} \approx C/T_{film}$. It turns out that the proportionality constant depends only weakly on n_f. The maximum of S_{OWG} is reached when T_{film} is close to the cutoff thickness:

$$T_{cutoff} = [(2\pi/\lambda)(n_f^2 - n_s^2)^{1/2}]^{-1} \arctan[(n_s^2 - n_c^2)^{1/2}/$$
$$(n_f^2 - n_s^2)^{1/2}] \qquad (2)$$

T_{cutoff} is nearly proportional to $1/(n_f - n_s)$, so that the maximum of S_{OWG} is approximately proportional to $(n_f - n_s)$ [14]. Large S_{OWG} are obtained with large $(n_f - n_s)$. Thin films with high refractive indexes deposited onto transparent substrates exhibit very high sensitivity, but they also usually show large losses of guided light [15], which is the dilemma that has been solved by the use of a thin-film composite OWG structure.

The relative sensitivity, S_{rel} of the Ag$^+$/K$^+$-ion-exchanged glass composite OWG, was observed as ca. 1300 times/cm for 633 nm; this values are 20–30 times as large as those observed in K$^+$-ion-exchanged glass OWG, and are slightly smaller than the calculated maximum value 1500 times/cm [28]. Table 1 lists the published reports, for each OWG, refractive indices, attenuation loss, and surface sensitivity.

3. Composite OWG for sensor applications

The application of integrated optical techniques in (bio-) chemical sensing has been subject of various research undertakings. These were motivated by the advantages that optical sensing techniques have over electrical methods, such as high sensitivity, immunity to electromagnetic interference, and safety in detection of combustible and explosive materials. In addition, the thin-film composite OWG is extremely sensitive to surface conditions, because the intensity of the evanescent wave at the guiding-film surface is very strong.

Fig. 6 shows a composite OWG sensor system. The composite OWG sensor device contained in a flow cell is mounted on a rotational stage equipped with X–Y–Z translation. A

Table 1
The refractive indices, attenuation loss α and the experimental (S_{OWG}) and theoretical (S_{rel}) surface sensitivity of the various OWG

| OWG	Refractive indices	Δn	S_{OWG} (cm^{-1})	S_{rel} (cm^{-1})	α (dB cm^{-1})	Reference
K$^+$-ion-exchanged glass OWG	1.52	0.008–0.02		50–100	>0.5	[28]
Ag$^+$/K$^+$ glass composite OWG	1.58/1.52 Ag$^+$/K$^+$	0.06	1500	1300	3–5	[16,17]
FePO$_4$ film/K$^+$ glass composite OWG	1.72/1.52 FePO$_4$/K$^+$	0.1	1.3×10^4	6.7×10^3	60–80	[15]
BTB film/K$^+$ glass composite OWG	1.69/1.52 BTB/K$^+$	0.17	4.7×10^3		5–6	[21]
PTA film/K$^+$ glass composite OWG	1.95/1.52 PTA/K$^+$	0.43	1.7×10^4	4.4×10^3	2–3	[19]
TiO$_2$ film/K$^+$ glass composite OWG	2.3/1.52 TiO$_2$/K$^+$	0.78	3.8×10^4		>5	[18]
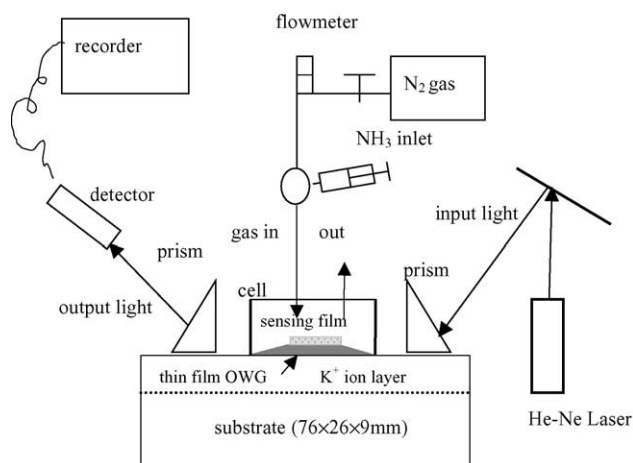
Fig. 6. Optical waveguide (OWG) gas sensor system and BTB doped thin-film/K$^+$-ion-exchanged glass composite optical waveguide [23].

He–Ne laser (633 nm) is used as a light source. The laser beam is injected into the composite OWG using a prism coupler (glass prism, $n = 1.75$, matching liquid diiodomethane, $n = 1.74$) and ejected at a second prism coupler. The intensity of the outgoing light (signal) is measured using a photomultiplier detector. From the point of view of optical principles, OWG (bio-) chemical sensors can be classified into absorption, refractive index change (scattering), fluorescence [29], and interference [30] measurements. Here we summarize our work on the development of sensors for gaseous ammonia (absorption) and immunoglobin G (refractive index change).

3.1. Ammonia sensor

OWG sensors based on absorption measurements have a simple structure and are easy to fabricate and use. They require the sensitive materials to yield a color change when the sensors are exposed to the environment containing the desired (bio-) chemical analytes.

The use of OWG to detect ammonia gas is usually based on the absorption of the evanescent field of the guided wave by pH-sensing dyes such as thymol blue (TB) [31], bromcresol purple (BCP) [13], and bromothymol blue (BTB) [20–23]. The sensing film of the indicator dye is coated onto the composite OWG surface (highly sensitive part). Depending on the concentration of ammonia, the indicator dye reversibly changes its color from yellow to blue, and absorbs the evanescent field of the guided light is the composite OWG sensitive layer.

A common method of fabricating ammonia sensors is to immobilize polymer films doped with pH-sensing dyes on the surface of OWG. This kind of optical ammonia sensor has relatively low sensitivity owing to a weak evanescent field and low concentration of dye in the sensing layers. By using pure dye film as the ammonia-sensing layer on a composite OWG instead of the dye-doped polymer layer we could avert these weak points and improve the performance of the sensor. To avoid high temperature decomposition of the or-

ganic reagents, we used a spin-coating thin-film preparation method to fabricate the pure BTB thin-film layers. Best results were obtained using acidic state BTB ethanol solutions. The fresh BTB film has a relatively smooth surface and high refractive index (1.69). It appears yellow and absorbs light of wavelength below 550 nm in air [21,22], but does not absorb the 633 nm He–Ne laser beam. In the presence of ammonia, the BTB film changes its color from yellow to blue ($\lambda_{max} = 624$ nm) [22], allowing absorption of the 633 nm evanescent wave on the composite OWG. Indeed, these characteristics of the BTB film make the He–Ne laser a good light source for the BTB film/TiO$_2$ film/K$^+$-ion-exchanged glass composite OWG ammonia sensor.

The propagation of the guided mode in this composite OWG was examined using prism coupling of a 633 nm He–Ne laser beam; the light streak in the region of the BTB film/TiO$_2$ film was wider and brighter than in the regions without coating. Such a light streak is a main characteristic of the composite OWGs and implies that the adiabatic transition of the guided mode between the K$^+$-ion-exchanged layer and the BTB film/TiO$_2$ film was realized at the tapered couplers. We found that the optimum BTB film thickness for the composite OWG ammonia sensor is about 45 nm. From theoretical calculations, it is clear that the sensitivity of composite OWG depends on the thickness of both the BTB and the TiO$_2$ film. The theoretical sensitivity of the composite OWG reaches its maximum value when the TiO$_2$ film thickness is 18–20 nm and the BTB film thickness is 45 nm; this result fully agrees with the experimental results mentioned above.

Fig. 7 shows an example for the reversible response of the BTB film/TiO$_2$ film/K$^+$-ion-exchanged glass composite OWG sensor to various concentration of ammonia vapor: When the composite OWG sensor was exposed to ammonia vapor, the output light intensity (signal) decreased rapidly and stabilized after a few seconds. Conversely, when ammonia was exhausted from the flow cell, the output light intensity fully returned to its primary level with pure nitrogen gas. Under the described experimental conditions, the composite OWG sensor achieved the desired detection limit of 1 ppt of ammonia, thereby exceeding the sensitivity of a dog's nose and any other sensors known so far.

Table 2 lists the theoretical sensitivity of the composite OWGs and the approximate detection limits. It can be seen that the detection limit of the sensors depends on the surface sensitivity of the composite OWG, and is improved by increasing the difference in refractive index between the thin film and the K$^+$-ion-exchanged layer.

3.2. Immunosensor

In OWG systems, signal attenuation may be caused not only by evanescent wave absorption but also by refractive index changes at the OWG surface. In biochemical affinity sensors, the chemically selective coating the OWG surface contains receptor molecules that selectively bind
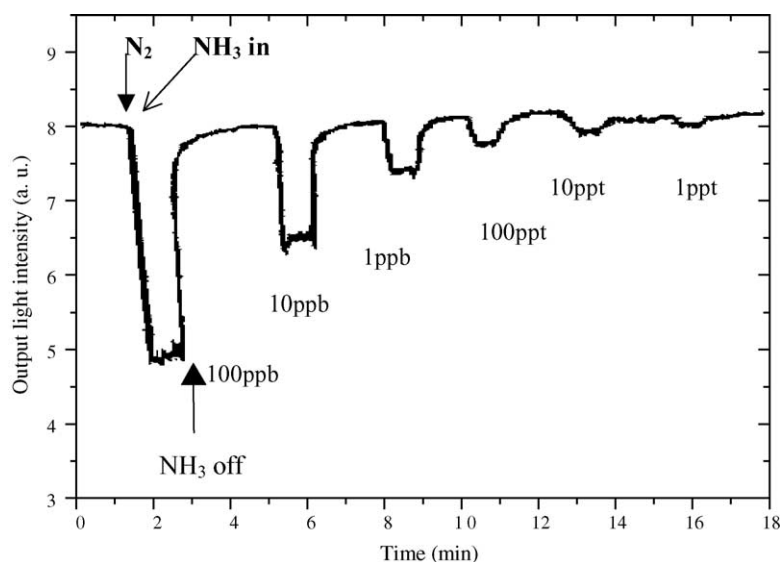
Fig. 7. Typical response of a BTB film/TiO$_2$ films/K$^+$-ion-exchanged glass composite OWG sensor when exposed to ammonia vapors in nitrogen. Arrow indicates the times when the ammonia vapor and pure nitrogen were injected into the flow cell [23].
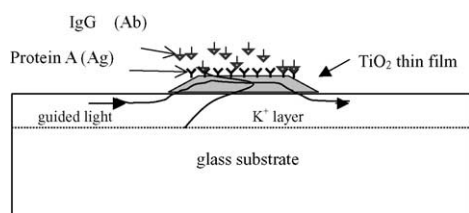

Fig. 8. Basic OWG sensor effect. Changes ΔN_{eff} of the effective refractive index N_{eff} of the guided mode are induced by changes of the refractive index distribution $n(z)$ in the vicinity of the waveguide surface [24].

certain ligands as analyte molecules (see Fig. 8). As a result, the refractive index of the medium near the OWG surface (antibody–antigen complex) is increased. As a result, the output light intensity (signal) decreases, because the intensity of the evanescent wave at the composite OWG surface becomes stronger, and more sensitive to the surface condition. Increases of the refractive index of the (composite OWG) sensing layer will cause changes in the propagation of the guided light. There is inevitable roughness on the film surface and scattering attenuation at the surface will increase when the electric field of the evanescent wave becomes stronger. Thus, the attenuation will become larger when the guided light propagates through the thin-film OWG [14].

By using the highly selective affinity reaction between IgG (glycoprotein immunoglobulin G, a major effector molecule of the humoral immune response in man, which accounts for about 75% of the total immunoglobulins in plasma of healthy individuals) and protein A (a highly stable surface receptor produced by *Staphylococcus aureus*, which is capable of binding the IgG) a sensor for immunoglobulin IgG was developed [33]. The sensing layer of protein A was coated onto the TiO$_2$ film/K$^+$-ion-exchanged glass composite OWG surface with (γ-aminopropyl) triethoxysilane. Aqueous solutions of IgG and NaCl were injected into the cell through separate injection ports (see Fig. 6; all measurements were carried out at room temperature).

Fig. 9 shows the OWG sensor response in distilled water, IgG solution (7 ng/cm^3) and NaCl solution. When the water was drained off, solutions of IgG in a phosphate buffer (pH 7) were injected into the cell. The output light intensity (signal) decreased and stabilized after a few minutes. When IgG bound to protein A was removed with a 0.5 mol dm^{-3} NaCl solution and distilled water, the output light intensity fully returned to its primary level.

The attenuation of the output intensity is here defined as $\alpha = 10 \log (P_{H_2O}/P_{IgG})$, where P_{H_2O} is the initial output light intensity, and P_{IgG} is the lowest point of the output

Table 2
Detection limits of ammonia sensors and theoretical sensitivities of (composite) OWGs

Ammonia sensors	Sensing film	Δn	S_{OWG} (times/cm)	Detection limit	Reference
K$^+$-ion-exchanged glass OWG	BTB + polymer	0.008	50	10 ppm	[32]
Ion-exchange in B-270 glass	BCP porous SiO$_2$			1 ppm	[13]
Ag$^+$/K$^+$ composite OWG	BTB + polymer	0.06	1500	100 ppb	[20]
BTB film/K$^+$ composite OWG	Pure BTB thin film	0.17	4.7×10^3	1 ppb	[21]
PTA film/K$^+$ composite OWG	Pure BTB thin film	0.43	1.7×10^4	1 ppb	[22]
TiO$_2$ film/K$^+$ composite OWG	Pure BTB thin film	0.78	3.8×10^4	1 ppt	[23]

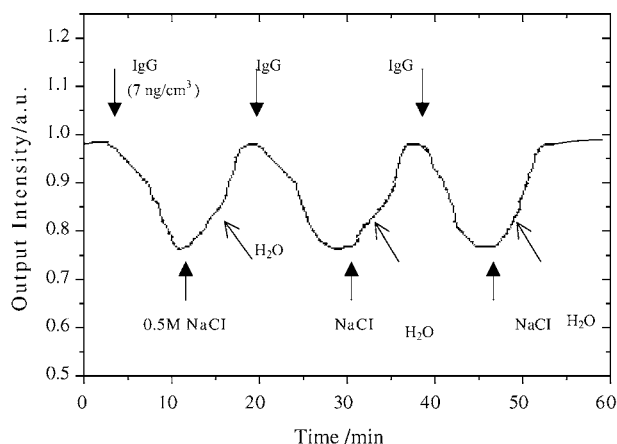BTB: bromothymol blue; BCP: bromcresol purple.

Fig. 9. A typical sensor response of the IgG sensor [24]. The IgG was removed by subsequently injecting aqueous NaCl and H_2O as indicated by the arrows.

light intensity, corresponding to before and after the injection of IgG in the flow cell, respectively. We found $\alpha = 2.9$–$0.4\,\text{dB}\,\text{cm}^{-1}$, corresponding to IgG concentrations of $7\,\mu\text{g/cm}^3$–$70\,\text{pg/cm}^3$. Under the described experimental conditions the composite OWG sensor can detect $70\,\text{pg/cm}^3$ of IgG easily (see Fig. 10).

The protein A-TiO_2 film/K^+-ion-exchanged glass composite OWG immunosensor is fast in response, reversible, and highly sensitive for IgG. In addition, the composite OWG sensor is simple in structure, which makes its fabrication easy and inexpensive.

3.3. Refractive index sensor

The sensitivity of the composite OWG to the refractive index n_c of the cladding layer can also be used to monitor n_c itself. As an example, a TiO_2 film/K^+-ion-exchanged glass composite OWG device has been developed for refractive index measurements [18]. Glycerin water solutions with concentrations of 0–100 wt% were used as the cladding
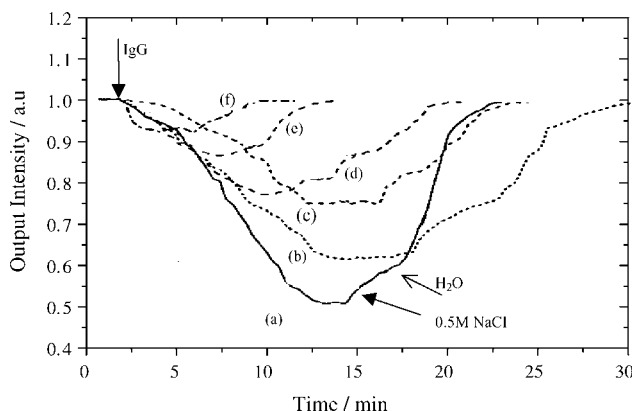

Fig. 10. Temporal response of the sensor to different concentrations of IgG. (a) $7\,\mu\text{g/cm}^3$, (b) $700\,\text{ng/cm}^3$, (c) $70\,\text{ng/cm}^3$, (d) $7\,\text{ng/cm}^3$, (e) $700\,\text{pg/cm}^3$, (f) $70\,\text{pg/cm}^3$ [24].

layer ($n_D^{20} = 1.33303$–1.47399). The intensity of the monitoring light became weaker, as expected, when the refractive index of the cladding layer increased while the cladding layer material was successively substituted from glycerin to water. The sensitivity of the sensor was found to be about 10^{-4}.

4. Conclusions

In this review, we described our recent results about the composite OWG method, which has high potentiality for the optical (bio-) chemical sensors and surface monitoring. We described the preparation of the composite OWG (bio-) chemical sensor with two thin guiding layers (BTB film/TiO_2 film). This composite OWG system proved to be fast in response and highly sensitive for ammonia. We demonstrated the immobilization of protein A on a waveguide surface. Even more importantly, monitoring of biochemical reactions such as immunoreactions (between antibodies and antigens), where one reaction partner is immobilized on the waveguide surface, was shown to be possible in real time. We also demonstrated the feasibility of direct affinity sensors and immunosensors with subnanomolar detection limits.

Composite OWG sensors have a low cost, simple structure and are easily fabricated. They may form the basis for extremely sensitive miniature devices in chemical or biological sensor applications. We would be delighted if our approach would stimulate further progress in this field.

References

[1] K. Itoh, A. Fujishima, J. Am. Chem. Soc. 110 (1988) 6267.
[2] K. Itoh, A. Fujishima, J. Phys. Chem. 92 (1988) 7043.
[3] P.L. Smock, T.A. Orofino, G.W. Wooten, W.S. Spencer, Anal. Chem. 51 (1979) 505.
[4] J.F. Guiliani, H. Wohltjen, N.L. Jarvis, Opt. Lett. 8 (1983) 54.
[5] P.M. Nellen, K. Tiefenthaler, W. Lukosz, Sens. Actuators 15 (1988) 285.
[6] R.V. Ramaswamy, R. Srivastava, J. Lightwave Technol. 6 (1988) 984.
[7] L. Yang, S.S. Saavedra, N.R. Armstrong, J. Hayes, Anal. Chem. 66 (1994) 1254.
[8] L. Yang, S.S. Saavedra, N.R. Armstrong, Anal. Chem. 68 (1996) 1834.
[9] M. Zourob, S. Mohr, B.J. Treves Brown, P.R. Fielden, M. McDonnell, N.J. Goddard, Sens. Actuators B 90 (2003) 296.
[10] H. Hisamoto, K.-H. Kim, Y. Manabe, K. Sasaki, H. Minamitani, K. Suzuki, Anal. Chim. Acta 342 (1997) 31.
[11] K.-H. Kim, H. Minamitani, H. Hisamoto, k. Suzuki, S.-W. Kang, Anal. Chim. Acta 343 (1997) 199.
[12] Y. Ren, P. Mormile, L. Petti, G.H. Cross, Sens. Actuators B 75 (2001) 76.
[13] R. Klein, E. Voges, Sens. Actuators B 11 (1993) 221.
[14] K. Itoh, M. Murabayashi, in: Council of Scientific Research Integration (Ed.), Trends in Physical Chemistry, 1, Research Trens. India, 1991, p. 179.
[15] K. Itoh, M. Madou, J. Appl. Phys. 69 (1991) 7425.
[16] K. Itoh, X.-M. Chen, M. Murabayashi, Chem. Lett. (1993) 1991.
[17] X.-M. Chen, K. Itoh, M. Murabayashi, Bull. Chem. Soc. Jpn. 68 (1995) 2823.

[18] X.-M. Chen, D.-K. Qing, K. Itoh, M. Murabayashi, Opt. Rev. 3 (1996) 351.

[19] A. Yimit, K. Itoh, Z.-M. Qi, M. Murabayashi, Electrochemistry 69 (2001) 182.

[20] X.-M. Chen, K. Itoh, M. Murabayashi, C. Igarashi, Chem. Lett. (1996) 103.

[21] Z.-M. Qi, A. Yimit, K. Itoh, M. Murabayashi, N. Matsuda, A. Takatsu, K. Kato, Opt. Lett. 26 (2001) 629.

[22] A. Yimit, K. Itoh, M. Murabayashi, Electrochemistry 69 (2001) 863.

[23] A. Yimit, K. Itoh, M. Murabayashi, Sens. Actuators B 88 (2003) 239.

[24] A. Yimit, X. Huang, Y. Xu, T. Amemiya, K. Itoh, Chem. Lett. (2003) 86.

[25] A.F. Milton, W.K. Burns, Appl. Opt. 14 (1975) 1207.

[26] T. Kudo, Nature 312 (1984) 537.

[27] K. Itoh, T. Okamaoto, S. Wakita, H. Niikura, M. Murabayashi, Appl. Organometal. Chem. 5 (1991) 295.

[28] K. Itoh, M. Murabayashi, K. Yamazaki, A. Fujishima, Chem. Lett. (1993) 283.

[29] Z.-M. Qi, K. Itoh, M. Murabayashi, H. Yanagi, J. Lightwave Technol. 18 (2000) 1106.

[30] J.C. Morey, N.J. Goddard, J.P. Lenney, R.D. Snook, P.R. Fielden, Sens. Actuators B 39 (1997) 212.

[31] S. Muto, A. Ando, T. Ochiai, H. Ito, H. Sawada, A. Tanaka, Jpn. J. Appl. Phys. 28 (1989) 125.

[32] C.R. Lavers, K. Itoh, S.C. Wu, M. Murabayashi, I. Mauchline, G. Stewart, T. Stout, Sens. Actuators B 69 (2000) 85.

[33] H. Muramatsu, K. Kajiwa, E. Tamiya, I. Karube, Anal. Chem. 59 (1987) 2760.